



Preparation of TiZrHfNbMo refractory high entropy alloy powder via hydrogen plasma-arc melting



Xiangyang Shen^a, Guishen Zhou^a, Feng Liu^a, Fuyu Dong^{a,*}, Yue Zhang^{a, **}, Xiaoguang Yuan^a, Binbin Wang^b, Liangshun Luo^b, Yanqing Su^b, Jun Cheng^{c,***}, Peter K. Liaw^d

^a School of Materials Science and Engineering, Shenyang University of Technology, Shenyang, 110870, China

^b School of Materials Science and Engineering, Harbin Institute of Technology, Harbin, 50001, China

^c Northwest Institute for Nonferrous Metal Research, Shaanxi Key Laboratory of Biomedical Metal Materials, Xian, 710016, China

^d Department of Materials Science and Engineering, The University of Tennessee, Knoxville, TN, USA

ARTICLE INFO

Keywords:

Refractory high-entropy alloy
Hydrogen plasma-arc melting
Powder technology
Particle
Microstructure

ABSTRACT

Refractory high-entropy alloys (RHEAs) are a new type of metal materials composed of four or more refractory elements. However, the melting point and liquid viscosity coefficient of RHEAs are high, which leads to low fluidity. Therefore, powders of such alloys are difficult to prepare by conventional methods. In this study, a new method called a hydrogen plasma-arc melting has been developed for the preparation of RHEA powders. Results show that the TiZrHfNbMo RHEA powders have single body-centered-cubic (BCC) structures, consisting of a large number of irregularly-shaped powders and small numbers of spherical powders. The average particle size of the powder was 66.97 μm . There is no obvious composition segregation on the surface and inside of the RHEA powders. In addition, this method greatly reduces the oxygen content of the powders.

1. Introduction

With progress in the science and technology of materials, a variety of new materials continue to emerge. High-entropy alloys (HEAs) have excellent physical and chemical properties, such as high hardness, great strength, and corrosion resistance [1–3]. Especially, due to their high-temperature strength and thermal stability, they are widely used in high-temperature resistant fields, such as in the nuclear and aerospace industries [4–7].

At present, there are two main preparation methods for HEAs powders [8,9]. One method is mechanical alloying, which is commonly used to prepare HEAs powders [10]. It is a process in which a highly deformed layer of particles containing a mixture of different elements is formed by interactions between alloy-powder particles and their interactions with high-energy balls in a ball mill. Although mechanical alloying has the advantages of simplicity and low cost, impurities are easily introduced, and pollution also spreads. The other method is the widely-used atomization method for preparing fine-metal spherical powder. In the powder preparation by atomization, high-speed gas/liquid flow acts on the

flowing molten metal, forming fine droplets, which then solidify into powder particles [11–13]. However, due to the high melting point, high liquid viscosity, and poor fluidity of HREAs, it is difficult to prepare this kind of powder by the conventional atomization method. In addition, some researchers have used a composite-plasma spheroidization method, which processes raw materials into fine powder and then spheroidizes the powder by plasma. For example, Park et al. [14] have prepared a spherical WTaMoNbV HEA powders by inductively-coupled thermal plasma spheroidization. Liu et al. [15] have prepared spherical ultrahard NbMoTaW refractory HEAs powders by spray drying and plasma spheroidization, showing a uniform particle-size distribution. The HEA powders present an overall single body-centered-cubic structure. However, this method usually requires multiple steps and special equipment, which is both time-consuming and harmful to energy conservation and environmental protection.

In present work, the MoNbHfZrTi RHEA powders were successfully prepared by hydrogen plasma-arc melting method. The crystalline structure, morphology, and elemental distribution of these RHEAs were characterized and analyzed. This method is expected to solve the

* Corresponding author.

** Corresponding author.

*** Corresponding author.

E-mail addresses: dongfuyu2002@163.com (F. Dong), yuezhang@sut.edu.cn (Y. Zhang), Chengjun_851118@126.com (J. Cheng).

problem that RHEA powers are difficult to prepare due to high melting point and high liquid viscosity coefficient and low fluidity.

2. Experimental methods

2.1. Powder preparation

It is well known that hydrogen embrittlement is a common phenomenon in nature, usually accompanied by fracture failure of materials [16]. In other words, hydrogen embrittlement has an irreversible negative effect on the mechanical properties of the alloy. In order to better understand, a schematic diagram of the mechanism of action of hydrogen on the alloy at high temperature was drawn, as shown in Fig. 1(a). The hydrogen atoms preferentially segregate at the grain boundary and reduce the interfacial bonding force [17]. In addition, high temperature accelerates the diffusion rate of hydrogen atoms, which not only occupies vacancies and voids, but also reacts with dislocations, eventually causing intragranular fracture. According to this principle, this study attempt to pulverize RHEA ingots by hydrogen embrittlement, and finally achieve the purpose of preparing powders. Hence, high-purity refractory metals, Ti, Zr, Hf, Nb, and Mo (purity $\geq 99.9\%$ weight percent), were provided by the Beijing Dream Material Technology Co., Ltd. (Beijing, China). The raw materials were melted into alloy ingots with uniform compositions in the Ar atmosphere. Then, the alloy ingot was melted in 15 % (volume percent) H_2/Ar atmosphere and 300 A current for 10 min to obtain the powder. After melting, the powder is cooled in the vacuum furnace for 8 min to avoid oxidation. The alloy powder attached to the copper tank and furnace wall were collected for characterization tests. Under the action of plasma, hydrogen atoms were ionized into hydrogen ions into the alloy ingot, as shown in Fig. 1(b). The number of hydrogen ions increases with the increase of melting time, resulting in the embrittlement of the alloy

ingot to form irregularly-shaped powders, as shown in Fig. 1(c). However, due to the high temperature in the arc column region, a small amount of irregularly-shaped powders located at this position quickly melted and condensed into spherical droplets under surface tension, forming spherical powder after contacting with the copper mold (Fig. 1(d)).

2.2. Microstructural characterizations

After hydrogen-plasma arc-melting, the alloy powder was gathered for characterization. An X-ray diffractometer (XRD, Shimadzu Corp., Kyoto, Japan) was used to analyze the crystalline structure of the powder, for which the scanning angle ranged over 20–100° and scanning speed 5°/min. The powder morphology and elemental distribution were observed and analyzed by scanning electron microscopy (SEM; FEI Q45, FEI Co., Hillsboro, OR, USA) equipped with an energy-dispersive spectrometer (EDS, Oxford Instruments plc, Abingdon, UK). The phase of the powder was analyzed by transmission electron microscopy (TEM, FEI Tecnai G2 F20, FEI Co.). Samples for TEM were prepared, using a focused ion beam (FIB; FEI Helios Nanolab 600i dual beam SEM, FEI Co.). In addition, the oxygen content of ingot and powder was detected by LECO ONH analyzer.

3. Results and discussion

Fig. 2(a) and (b) present the SEM images of as-cast TiZrHfNbMo RHEA. It can be seen that the alloy exhibits a typical dendritic structure, which is caused by composition segregation. Several studies have shown that the solidification sequence is different due to the large difference in the melting point of the elements [18,19]. During the cooling process, the elements with high melting point are first enriched to form dendritic arms, while the elements with low melting point are pushed to the

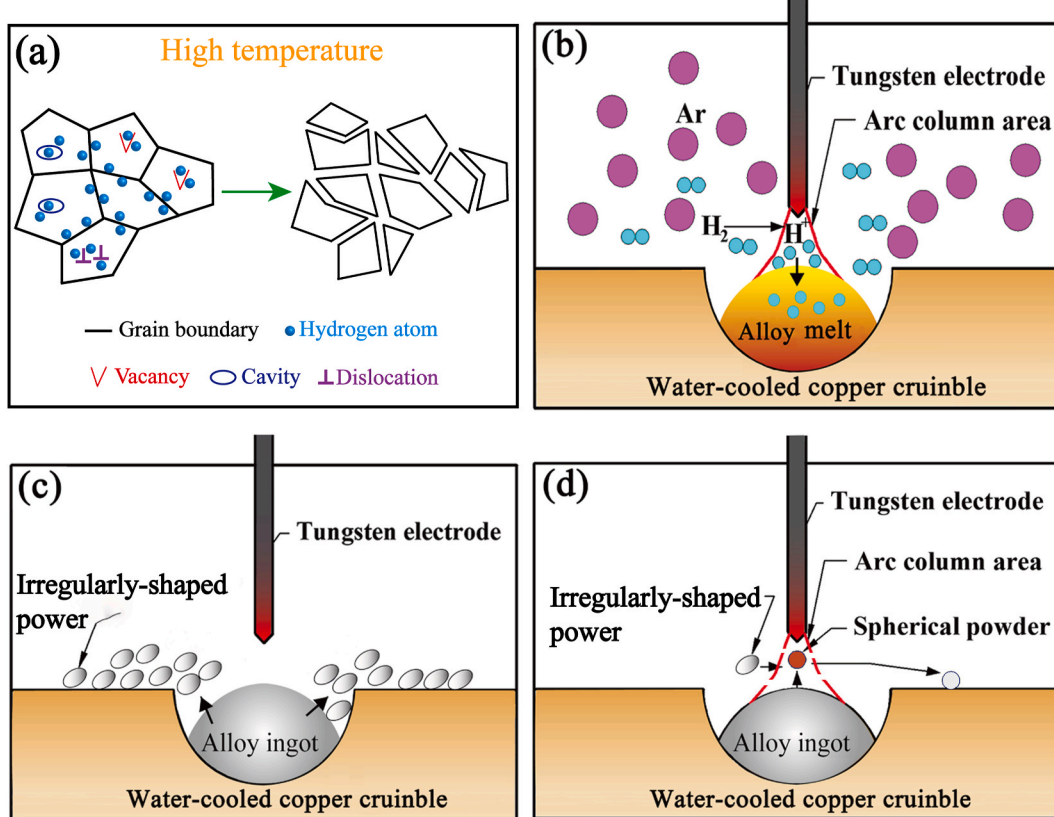
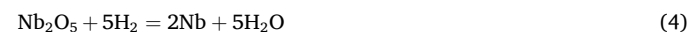


Fig. 1. Schematic diagram of (a) hydrogen embrittlement at high temperature, (b) hydrogen absorption, (c) irregularly-shaped powders, and (d) spherical powders formation.

surrounding region to form interdendritic. After hydrogen plasma-arc treatment, RHEA powders are mainly composed of irregular blocks and a small amount of spheres, as shown in Fig. 2(c) and (d). The XRD patterns of the RHEA ingots and powders are shown in Fig. 2(e). It can be confirmed that RHEA powders still maintains a single BCC structure, and no other intermetallic compounds are formed. The particle-size distribution of the powders was statistically analyzed using an MIPAR software, as shown in Fig. 2(f). The results show that the sizes of most of the powder were between 20 and 100 μm and a small amount of $>140 \mu\text{m}$, with an average particle size calculated to be 66.97 μm .

Fig. 3(a) and (b) show the elemental distribution of irregularly-shaped and spherical RHEA powders, respectively. It can be concluded that the powders have no obvious composition segregation. Fig. 4 shows the element content in the square region in the two shapes of powders. The actual composition floats slightly up and down the nominal composition, which further indicates that the element distribution is relatively uniform. Since the content of impurity elements will affect the purity and properties of the powder, especially the oxygen with high affinity with TiZrHfNbMo RHEA, its content should be strictly controlled. No information about oxygen is obtained in SEM-EDS, which could be attributed to the fact that the equipment could not be accurately identified due to the low oxygen content, and it could also be confirmed from the XRD pattern that no other diffraction peaks appeared (Fig. 2(e)). Therefore, the oxygen content of RHEA ingot and powder was determined by LECO ONH analyzer to be 418 and 293 ppm,

respectively. The oxygen content of the powder after hydrogen plasma-arc melting is greatly reduced, which indicates that the process can decrease oxygen pollution. The decrease of oxygen content is mainly due to the following three reasons: First, before melting, the titanium ingot used to ignite the arc will absorb a certain amount of oxygen. Second, the high-purity argon environment effectively reduces the production of oxides during the melting process. Last but not least, high temperature will accelerate the reaction of hydrogen with oxides, and the product water will evaporate rapidly [20]. Previous studies reveal that the sheath gas of hydrogen is not only a good deoxidizer, but also promotes the evaporation of water on the powder surface by high temperature plasma to prevent oxidation [21]. Here, the reaction of hydrogen with metal oxides can be expressed as



To further determine the crystal structure of the RHEA powders, the samples were cut in the red square region by the FIB technique for TEM

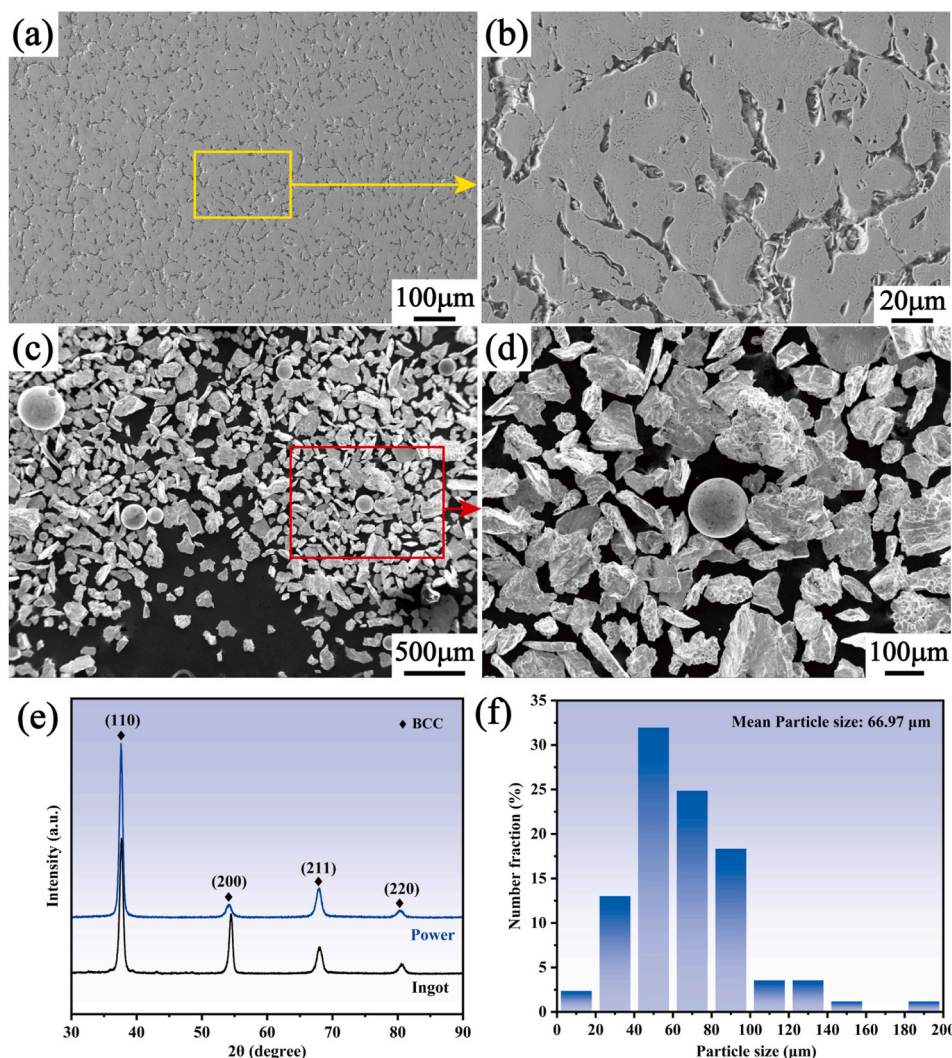


Fig. 2. SEM images: (a) ingot, (b) enlarged image of (a), (c) powders, (d) enlarged image of (c). (e) XRD pattern of the ingot and powders. (f) Particle size distribution.

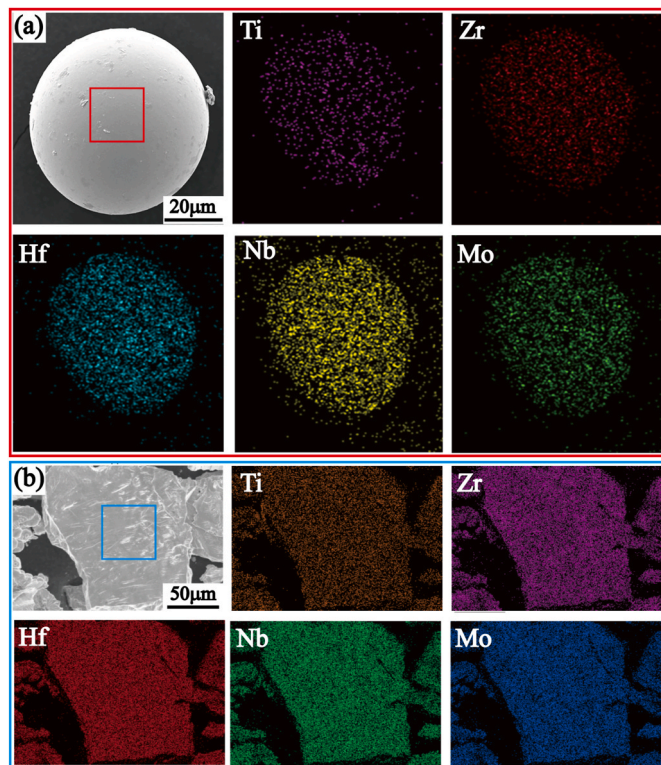


Fig. 3. SEM images and its EDS mapping of (a) spherical and (b) irregularly-shaped powders.

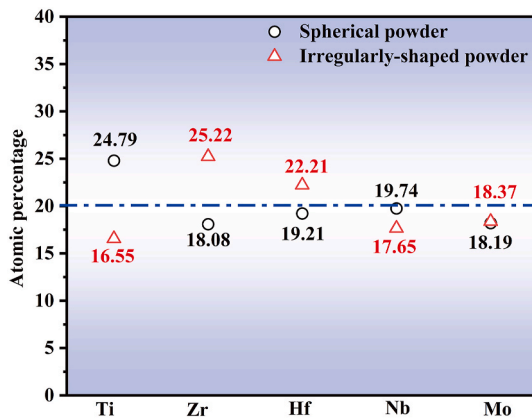


Fig. 4. Atomic percentage of elements in spherical and irregularly-shaped powders.

analysis, as shown in Fig. 5(a). The selected area electron diffraction (SAED) pattern (Fig. 5(b)) show that the RHEA powders have a single BCC structure, which was consistent with XRD results. The TEM-EDS shows that the elements inside the RHEA powder are uniformly distributed, as shown in Fig. 5(c).

By microscopic morphology characterization, it can be found that the RHEAs powders have smaller particle size and larger specific surface area than the bulks, which will make them more flexible and plastic during processing and manufacturing. In addition, RHEAs powders have unique microstructure and excellent performance characteristics, which lead to their broad application prospects in the fields of aerospace, electronic equipment, biomedicine and hydrogen storage [22]. This preparation method can solve the deficiencies of as-cast bulk RHEAs, such as serious composition segregation, coarse grains and many defects [23]. It should be noted that the powder prepared by this method can

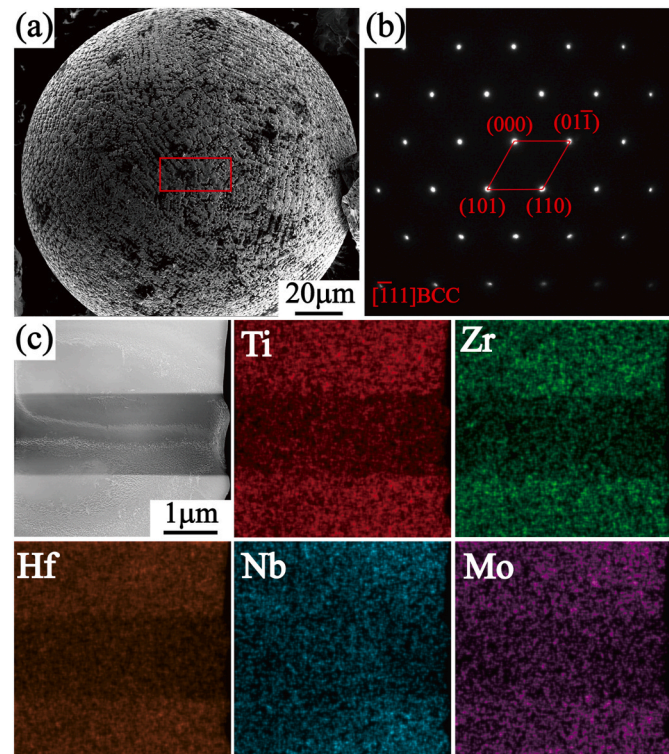


Fig. 5. (a) SEM image of spherical powder, (b) the SAED pattern, and (c) TEM image and its EDS mapping.

achieve high sphericity through subsequent plasma spheroidization, which is expected to provide high-quality raw materials for additive manufacturing.

4. Conclusions

In summary, a low-cost method for preparing RHEA powders are developed. The TiZrHfNbMo RHEA powders were successfully prepared by this method and systematically characterized. The results show that the powders have a single BCC structure. The powders are composed of a large number of irregular shapes and a small amount of spheres. The powder particle sizes were mostly between 40 and 100 μm , with an average particle size is 66.97 μm . There is no obvious element segregation and oxidation phenomenon in the powder. Therefore, hydrogen-plasma arc melting is a potential new method for preparing RHEA powders.

CRediT authorship contribution statement

Xiangyang Shen: Writing – review & editing, Writing – original draft, Visualization, Resources, Methodology, Conceptualization. **Guishen Zhou:** Writing – review & editing, Methodology, Conceptualization, Formal analysis. **Feng Liu:** Validation, Supervision, Resources, Investigation, Data curation. **Fuyu Dong:** Writing – review & editing, Project administration, Funding acquisition, Formal analysis. **Yue Zhang:** Supervision, Funding acquisition, Data curation. **Xiaoguang Yuan:** Methodology, Formal analysis. **Binbin Wang:** Software, Conceptualization. **Liangshun Luo:** Methodology, Investigation. **Yanqing Su:** Formal analysis, Conceptualization. **Jun Cheng:** Validation, Funding acquisition, Conceptualization. **Peter K. Liaw:** Formal analysis, Conceptualization.

Declaration of competing interest

We declare that we have no financial and personal relationships with

other people or organizations that can inappropriately influence our work, there is no professional or other personal interest of any nature or kind in any product, service and/or company that could be construed as influencing the position presented in, or the review of, the manuscript entitled “Preparation of TiZrHfNbMo refractory high entropy alloy powder via hydrogen plasma-arc melting”.

Data availability

Data will be made available on request.

Acknowledgments

The present work was supported by National Natural Science Foundation of China (No. 52271249), Natural Science Foundation of Liaoning Province (No. 2023JH2/101700276), The Grant Plan for Young and Middle-aged Innovation Scientists of Shenyang Government (No. RC210058), Basic Scientific Research Project of Education Department of Liaoning Province (No. LJKMZ20220466), Key Research and Development Program of Shaanxi (No. 2023-YBGY-488) and Xi'an Talent Plan (XAYC240016). Project supported by State Key Laboratory of Powder Metallurgy, Central South University, Changsha, China. PKL very much appreciates the supports from (1) the National Science Foundation (DMR-1611180, 1809640, and 2226508) and (2) the Army Research Office (W911NF-13-1-0438 and W911NF-19-2-0049).

References

- [1] D.B. Miracle, O.N. Senkov, A critical review of high entropy alloys and related concepts, *Acta Mater.* 122 (2017) 448–511.
- [2] X. Yan, Y. Zhang, Functional properties and promising applications of high entropy alloys, *Scripta Mater.* 187 (2020) 188–193.
- [3] J.-W. Yeh, S.-J. Lin, Breakthrough applications of high-entropy materials, *J. Mater. Res.* 33 (2018) 3129–3137.
- [4] D. Hua, Q. Zhou, Y. Shi, S. Li, K. Hua, H. Wang, S. Li, W. Liu, Revealing the deformation mechanisms of (110) symmetric tilt grain boundaries in CoCrNi medium-entropy alloy, *Int. J. Plast.* 171 (2023) 103832.
- [5] Y. Ren, Q. Zhou, D. Hua, Z. Huang, Y. Li, Q. Jia, P. Gumbsch, C. Greiner, H. Wang, W. Liu, Wear-resistant CoCrNi multi-principal element alloy at cryogenic temperature, *Sci. Bull.* 69 (2024) 227–236.
- [6] Z. Guo, X. Shen, F. Liu, J. Guan, Y. Zhang, F. Dong, Y. Wang, X. Yuan, B. Wang, L. Luo, Y. Su, J. Cheng, Microstructure and mechanical properties of Al_x (TiZrTa_{0.7}NbMo) refractory high-entropy alloys, *J. Alloys Compd.* 960 (2023) 170739.
- [7] F. Dong, Y. Yuan, W. Li, Y. Zhang, P.K. Liaw, X. Yuan, H. Huang, Hot deformation behavior and processing maps of an equiatomic MoNbHfZrTi refractory high entropy alloy, *Intermetallics* 126 (2020) 106921.
- [8] S.-M. Chiu, T.-T. Lin, R.K. Samy, N.G. Kipkirui, Y.-Q. Lin, J.-T. Liang, S.-H. Chen, Investigation of phase constitution and stability of gas-atomized Al0.5CoCrFeNi2 high-entropy alloy powders, *Mater. Chem. Phys.* 275 (2022) 125194.
- [9] A. Ostovari Moghaddam, N.A. Shaburova, M.N. Samodurova, A. Abdollahzadeh, E. A. Trofimov, Additive manufacturing of high entropy alloys: a practical review, *J. Mater. Sci. Technol.* 77 (2021) 131–162.
- [10] Y. Qiao, Y. Tang, S. Li, Y. Ye, X. Liu, L. Zhu, S. Bai, Preparation of TiZrNbTa refractory high-entropy alloy powder by mechanical alloying with liquid process control agents, *Intermetallics* 126 (2020) 106900.
- [11] C.Y. Cui, H.H. Xu, F.Y. Ye, J. Yang, X.G. Cui, Microstructure evolution and characteristics of laser cladding with pre-placed powder lightweight refractory Nb_xMo_{0.5}Ti_{1.5}Ta_{0.2}Cr high-entropy alloy, *Intermetallics* 167 (2024) 108229.
- [12] S. Mohammadi, F. Akhlaghi, Effect of Al content on the microstructure and mechanical alloying behavior of AlCoCuMnNi and Al0.25CoCuMnNi high entropy powders, *Mater. Chem. Phys.* 313 (2024) 128768.
- [13] Y. Lee, C. Nagarjuna, J.-W. Song, K.Y. Jeong, G. Song, J. Lee, J.-H. Lee, S.-J. Hong, Powder characteristics of Al_{0.5}CoCrFeMnNi high-entropy alloys fabricated by gas atomisation method, *Powder Metall.* 64 (2021) 219–227.
- [14] J.-M. Park, J.-W. Kang, W.-H. Lee, S.Y. Lee, S.-H. Min, T.K. Ha, H.-K. Park, Preparation of spherical WTaMoNbV refractory high entropy alloy powder by inductively-coupled thermal plasma, *Mater. Lett.* 255 (2019) 126513.
- [15] B. Liu, H. Duan, L. Li, C. Zhou, J. He, H. Wu, Microstructure and mechanical properties of ultra-hard spherical refractory high-entropy alloy powders fabricated by plasma spheroidization, *Powder Technol.* 382 (2021) 550–555.
- [16] X. Li, J. Yin, J. Zhang, Y. Wang, X. Song, Y. Zhang, X. Ren, Hydrogen embrittlement and failure mechanisms of multi-principal element alloys: a review, *J. Mater. Sci. Technol.* 122 (2022) 20–32.
- [17] H. Wang, Z. Niu, C. Chen, H. Chen, X. Zhu, F. Zhou, X. Zhang, X. Liu, Y. Wu, S. Jiang, Powder production of an equimolar NbTaTiZr high-entropy alloy via hydrogen embrittlement, *Mater. Char.* 193 (2022) 112265.
- [18] S.H. Chen, J.S. Zhang, S. Guan, T. Li, J.Q. Liu, F.F. Wu, Y.C. Wu, Microstructure and mechanical properties of WNbMoTaZrx (x = 0.1, 0.3, 0.5, 1.0) refractory high entropy alloys, *Mater. Sci. Eng.* 835 (2022) 142701.
- [19] X. Shen, Z. Guo, F. Liu, F. Dong, Y. Zhang, C. Liu, B. Wang, L. Luo, Y. Su, J. Cheng, X. Yuan, P.K. Liaw, Microstructural evolution and mechanical behavior of novel TiZrTaxNbMo refractory high-entropy alloys, *J. Alloys Compd.* 990 (2024) 174459.
- [20] Y. Xia, J. Zhao, Z. Dong, X. Guo, Q. Tian, Y. Liu, A novel method for making Co-Cr-Mo alloy spherical powder by granulation and sintering, *JOM* 72 (2020) 1279–1285.
- [21] M. Xia, Y. Chen, K. Chen, Y. Tong, X. Liang, B. Shen, Synthesis of WTaMoNbZr refractory high-entropy alloy powder by plasma spheroidization process for additive manufacturing, *J. Alloys Compd.* 917 (2022) 165501.
- [22] B. Zhang, Y. Huang, Z. Dou, J. Wang, Z. Huang, Refractory high-entropy alloys fabricated by powder metallurgy: progress, challenges and opportunities, *J. Sci.: Advanced Materials and Devices* 9 (2024) 100688.
- [23] W. Xiong, A.X.Y. Guo, S. Zhan, C.-T. Liu, S.C. Cao, Refractory high-entropy alloys: a focused review of preparation methods and properties, *J. Mater. Sci. Technol.* 142 (2023) 196–215.